BIOCHEMISTRY
including biophysical chemistry & molecular biology

Article

pubs.acs.org/biochemistry

Structure–Function Analysis of the Two-Peptide Bacteriocin Plantaricin EF

Bie Ekblad,*[,†] Panagiota K. Kyriakou,[‡] Camilla Oppegård,[†] Jon Nissen-Meyer,[†] Yiannis N. Kaznessis,[‡] and Per Eugen Kristiansen*[,†]

[†]Department of Biosciences, University of Oslo, P.O. Box 1066, Blindern, 0316 Oslo, Norway

[‡]Department of Chemical Engineering and Materials Science, University of Minnesota, Minneapolis, Minnesota 55455, United States

Supporting Information

ABSTRACT: Plantaricin EF is a two-peptide bacteriocin that depends on the complementary action of two different peptides (PlnE and PlnF) to function. The structures of the individual peptides have previously been analyzed by nuclear magnetic resonance spectroscopy (Fimland, N. et al. (2008), *Biochim. Biophys. Acta 1784*, 1711−1719), but the bacteriocin structure and how the two peptides interact have not been determined. All two-peptide bacteriocins identified so far contain GxxxG motifs. These motifs, together with GxxxG-like motifs, are known to mediate helix−helix interactions in membrane proteins. We have mutated all GxxxG and GxxxG-like motifs in PlnE and PlnF in order to determine if any of these motifs are important for antimicrobial activity and thus possibly for interactions between PlnE and PlnF. Moreover, the aromatic amino acids Tyr and Trp in PlnE and PlnF were substituted, and four fusion polypeptides were constructed in order to investigate the relative orientation of PlnE and PlnF in target cell membranes. The results obtained with the fusion polypeptides indicate that PlnE and PlnF interact in an antiparallel manner and that the C-terminus of PlnE and N-terminus of PlnF are on the outer part of target cell membranes and the N-terminus of PlnE and C-terminus of PlnF are on the inner part. The preference for an aromatic residue at position 6 in PlnE suggests a positioning of this residue in or near the membrane interface on the cells inside. Mutations in the GxxxG motifs indicate that the G_5xxxG_9 motif in PlnE and the $S_{26}xxxG_{30}$ motif in PlnF are involved in helix−helix interactions. Atomistic molecular dynamics simulation of a structural model consistent with the results confirmed the stability of the structure and its orientation in membranes. The simulation approved the anticipated interactions and revealed additional interactions that further increase the stability of the proposed structure.

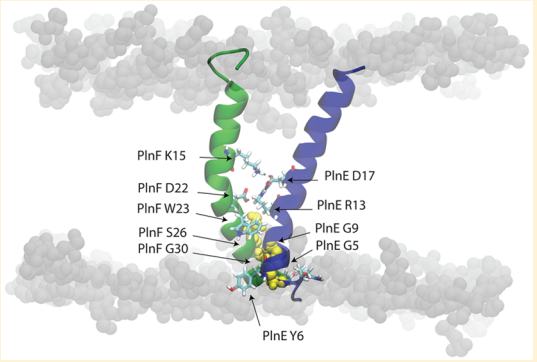

Production of antimicrobial peptides (AMPs) is an ancient and effective defense used by a wide variety of organisms to fight pathogens.[1,2] AMPs produced by bacteria, often referred to as bacteriocins, are especially potent; they are active at pico- to nanomolar concentrations, whereas AMPs of eukaryotes are active at micromolar concentrations.[3] Bacteriocins produced by lactic acid bacteria (LAB) are of special interest because of their generally recognized as safe (GRAS) status. These bacteriocins are divided into two main classes: the class-I lantibiotics that contain post-translationally modified lanthionine residues and the class-II non-lantibiotics that do not contain extensive modifications.[3,4] The class-II bacteriocins may be further divided into four subclasses: the class-IIa pediocin-like bacteriocins that have similar amino acid sequences, the class-IIb two-peptide bacteriocins that consists of two different peptides, the class-IIc cyclic bacteriocins, and the class-IId noncyclic one-peptide non-pediocin-like bacteriocins.[3,4]

Plantaricin EF is a class-IIb two-peptide bacteriocin that consists of the 33-residue PlnE and the 34-residue PlnF peptides, both of which are required in about equimolar amounts in order to obtain maximal antimicrobial activity.[5,6] The genes encoding PlnE and PlnF are next to each other in the same operon, along with the gene encoding the immunity protein that protects the plantaricin EF producer from being killed by the bacteriocin.[7] As is the case for all two-peptide bacteriocins whose mode of action has been studied, plantaricin EF renders the membranes of target cells permeable to small molecules, which eventually leads to cell death.[8,9] The high potency of two-peptide bacteriocins suggests that these bacteriocins act by binding to a specific membrane protein (a bacteriocin receptor), where the interaction between bacteriocin and receptor protein leads to membrane leakage and cell death.[3,10] UppP, a membrane-spanning protein involved in cell wall synthesis, has been identified as the receptor for the two-peptide bacteriocin lactococcin G and presumably the related two-peptide bacteriocins enterocin 1071 and lactococcin Q,[11] and a putative amino acid transporter was recently identified as

Received: June 10, 2016
Revised: August 16, 2016
Published: August 18, 2016

DOI: 10.1021/acs.biochem.6b00588
Biochemistry 2016, 55, 5106−5116

a possible target for the two-peptide bacteriocin plantaricin JK.[12]

Structural studies using circular dichroism (CD) and nuclear magnetic resonance (NMR) spectroscopy have been carried out on three two-peptide bacteriocins, namely, lactococcin G, plantaricin EF, and plantaricin JK.[6,13−16] The CD studies showed that all the peptides are unstructured in aqueous solutions and that structuring is first induced when the peptides come in contact with membrane-like entities. Furthermore, the two complementary peptides from each of these three two-peptide bacteriocins induced structuring in each other, indicating that the two peptides of two-peptide bacteriocins interact with each other and thus function as one unit upon contact with target membranes.[6,13] The NMR studies were performed on individual peptides in a hydrophobic or membrane-mimicking environment and revealed that the six peptides from the three two-peptide bacteriocins formed mainly α-helices with some flexible or somewhat unstructured parts, often in the N- and/or C-terminal regions.[14−16] Molecular dynamics (MD) simulation of plantaricin EF on the surface of a model lipid bilayer revealed persistent structural regions and interaction with the bilayer.[17]

Interestingly, all two-peptide bacteriocins that have been identified contain GxxxG motifs.[18,19] This motif, along with the GxxxG-like motifs such as AxxxA and SxxxS, are known to mediate helix−helix interactions in membrane proteins.[20−23] When part of an α-helix, the two glycine residues in GxxxG motifs will appear on the same side of the helix and form a flat interaction surface. When two α-helices contain GxxxG motifs, such interaction surfaces allow for close contact between the two helices, enabling extensive interhelical van der Waals interactions and formation of stabilizing backbone Cα−H···O hydrogen bonds.[20−22] On the basis of the high frequency of GxxxG motifs in two-peptide bacteriocins and the predominant helical structure of two-peptide bacteriocins whose structures have been analyzed, it has been proposed that many, if not all, two-peptide bacteriocins form parallel or antiparallel transmembrane helix−helix structures that are stabilized by GxxxG motifs.[3,18,19,24] NMR-structural characterization of the individual peptides that constitute the two two-peptide bacteriocins lactococcin G and plantaricin JK combined with extensive site-directed mutagenesis studies indicate that this is the case for these two bacteriocins (along with the lactococcin G homologues lactococcin Q and enterocin 1071).[15,19,25,26] MD simulation of the structure of the two-peptide bacteriocin plantaricin S indicates that this is probably also the case for plantaricin S.[24]

It has been proposed that the two peptides (PlnE and PlnF) of plantaricin EF form a parallel or antiparallel transmembrane helix−helix structure that is partly stabilized by GxxxG and/or GxxxG-like motifs.[14] PlnE contains two GxxxG motifs (G_5xxxG_9 and G_{20}xxxG_{24}) and two GxxxG-like motifs (A_{23}xxxG_{27} and G_{27}xxxS_{31}), and PlnF contains one GxxxG motif (G_{30}xxxG_{34}) and two GxxxG-like motifs (A_{17}xxxA_{21} and S_{26}xxxG_{30}).

Here we have analyzed the effect of substituting the various small amino acids (Gly, Ala, and Ser) in these motifs to see if any of these motifs are important for antimicrobial activity and hence interactions between PlnE and PlnF. Aromatic amino acids Tyr and Trp were also substituted, and four fusion polypeptides were constructed in order to investigate the relative orientation of PlnE and PlnF in target cell membranes. We further investigated the behavior of various peptide analogues in a model membrane environment through atomistic MD simulations. We propose a structural model of plantaricin EF that is consistent with the mutation results and MD analysis.

EXPERIMENTAL SECTION

Bacterial Strains and Growth Conditions. *Lactobacillus plantarum* C11 was grown overnight at 30 °C without agitation in de Man-Rogosa-Sharpe (MRS) medium (Oxoid). *Escherichia coli* DH5α and BL21(DE3) cells were used for plasmid amplification and production of fusion polypeptides, respectively. The cells were grown at 37 °C in lysogeny broth (LB) medium in baffled flasks with vigorous agitation. The medium contained either 150 μg/mL erythromycin for selection of the plasmids pPlnE100/pPlnF100 or 100 μg/mL ampicillin for selection of pET22b(+) and pGEM-T Easy Vector derivatives. For growth of *E. coli* DH5α on agar plates, the LB medium was solidified with 1.5% (w/v) agar.

Lactobacillus sakei Lb790, containing pSAK20 and either pPlnE100 or pPlnF100, was used for production of, respectively, PlnE or PlnF and their mutated variants. The plasmids pSAK20 and pPlnE100/pPlnF100 contain a marker for chloramphenicol and erythromycin resistance, respectively, and the cells were consequently grown (30 °C without agitation) in MRS medium containing 10 μg/mL of each antibiotic.

The indicator strains used in the bacteriocin activity assays were *Lactobacillus viridescens* NCDO 1655, *Lactobacillus curvatus* LTH 1174, *Pediococcus pentosaceus* NCDO 990, and *Pediococcus acidilactici* NCDO 521. All strains were grown at 30 °C in MRS medium without agitation.

DNA Isolation. Genomic DNA from *L. plantarum* C11 was isolated using the QIAGEN DNeasy Tissue kit according to protocol. Plasmids were isolated from *E. coli* DH5α cells using the Macherey-Nagel NucleoSpin Plasmid kit.

A Two-Plasmid Expression System for Production of Bacteriocins. A two-plasmid expression system[27,28] consisting of pSAK20 and the pLPV111-derived plasmids pPlnE100 or pPlnF100 was used to produce wild type and mutant variants of PlnE and PlnF. The two plasmids were introduced into the bacteriocin-deficient strain *L. sakei* Lb790. pSAK20 contains the *orf4-sapKRTE* operon needed for activation of the sakacin A promoter and processing and export of the bacteriocin.[27,28] pPlnE100 and pPlnF100 contain the genes encoding PlnE or PlnF, respectively, and PlnI (the plantaricin EF immunity protein), and the genes are placed under the control of the sakacin A promoter. The *plnE*- and *plnF*-genes are fused to the sakacin P leader sequence. Previous studies have demonstrated that the sakacin A secretion machinery encoded in pSAK20 recognizes both the sakacin A and sakacin P leader peptides equally efficient.[28]

All primers used for creation of pPlnE100 and pPlnF100 are listed in Table S1 in the Supporting Information.

For construction of the pPlnF100 plasmid, the plasmid pLT100α (a pLPV111-derivate used for expression of lactococcin Gα[26]) was used as a template for amplification of the sakacin A promoter region and the sakacin P leader sequence using the primers PlnFA and SakPB. The resulting PCR product (Megaprimer 1F) contains the restriction site for *Mlu*I, the sakacin A promoter, the sakacin P leader sequence as well as a tail complementary to the beginning of the *plnF*-gene. In the following PCR reaction, genomic DNA from *L. plantarum* C11 was used as template to amplify the *plnF*- and

DOI: 10.1021/acs.biochem.6b00588
Biochemistry 2016, 55, 5106−5116

plnI-genes using the primers PlnEFimm and Megaprimer 1F. The PCR product (flanked by restriction sites for *Mlu*I and *Cla*I) was subcloned into the pGEM-T Easy Vector due to incomplete restriction digestion, and the restriction site for *Cla*I was changed into an *Xba*I restriction site by use of the QuikChange site-directed mutagenesis method and the primers PlnEFXbaIF and PlnEFXbaIR (Table S1, Supporting Information). The fragment was subsequently cloned into the *Mlu*I and *Xba*I sites of pLPV111, resulting in pPlnF100.

The pPlnE100 plasmid was constructed in a similar manner. Primers PlnEC and Megaprimer 1E (containing the sakacin A promoter, the sakacin P leader sequence and the beginning of *plnE*) were used to amplify the *plnE*-gene. The resulting PCR product (Fragment 1) also contains the beginning of *plnI*. The *plnI*-gene and the end of the *plnE*-gene were amplified in a separate PCR reaction using primers PlnEFimmstart and PlnEFimm (Fragment 2). Fragment 1 and Fragment 2 were spliced by PCRSOEing.[29] The spliced PCR product was amplified by adding the two external primers PlnEFimm and SakPB. The final PCR product consists of the entire *plnI*-gene, the *plnE*-gene fused to the leader sequence of sakacin P, and the sakacin A promoter region, flanked by the restriction sites *Mlu*I and *Cla*I. The PCR product was subcloned into the pGEM-T Easy Vector due to incomplete restriction digestion. Finally, the fragment was cloned into the *Mlu*I and *Cla*I sites of pLPV111 resulting in pPlnE100.

Preparation of Competent Cells and Cell Transformation. *E. coli* cells were made competent by the $CaCl_2$-method (protocol II), basically as described by Sambrook et al.[30] The plasmids were introduced into *E. coli* DH5α cells according to the QuikChange site-directed mutagenesis protocol.[31] Preparation of competent *L. sakei* Lb790/pSAK20 cells and transformation were performed as previously described by Aukrust et al. (procedure 2).[32]

Site-Directed Mutagenesis and DNA Sequencing. In order to introduce point mutations in *plnE* and *plnF*, Quik Change site-directed mutagenesis was performed according to manufacturer's protocol.[31]

The DNA sequences of all the mutated plasmids were verified by DNA sequencing using an ABI PRISM 3730 DNA Analyzer and a BigDye Terminator v3.1 Cycle Sequencing kit.

Production and Purification of Peptides. The two-plasmid expression system described above was used for the production of wild type and mutant variants of PlnE and PlnF.

The peptides were purified from 1 L overnight cultures, basically as previously described.[33] The overnight cultures were applied directly to a cation exchange column equilibrated with 20 mM phosphate buffer (pH 6). The column was washed with 100 mL of the phosphate buffer before the peptides were eluted in 40 mL of 20 mM phosphate buffer (pH 6) containing 1 M NaCl and 20% (v/v) 2-propanol. The eluate was sterile-filtrated through a 0.20 μm nonpyrogenic sterile filter (Sarstedt) and subsequently diluted 4-fold with H_2O/0.1% (v/v) trifluoroacetic acid (TFA) and applied to a reverse phase column (3 mL RESOURCE RPC, GE Healthcare). The peptides were eluted with a linear 2-propanol-gradient containing 0.1% TFA. The absorbance at 280 and 214 nm was recorded as a function of mL eluent.

The molecular masses of the peptide variants were confirmed by MALDI-TOF mass spectrometry at the MS/Proteomics Core Facility at the Department of Chemistry, Biotechnology and Food Science, Norwegian University of Life Sciences. Because of the relatively weak absorbance at 280 nm (only one Tyr residue in the PlnE-peptide), the relative amount of peptides added to the bacteriocin activity measurements was estimated based on the absorbance peak at 214 nm obtained after purifying the peptides on a reverse phase column.

Some mutant peptides were ordered synthetically from GenScript. The synthetic peptides were ordered with a purity of >80% and dissolved in 40% 2-propanol upon arrival. The absorption was measured spectrophotometrically at 280 nm, and the concentration was estimated based on the molar extinction coefficients of the amino acids Tyr (ε_{280} = 1200 M^{-1} cm^{-1}) and Trp (ε_{280} = 5560 M^{-1} cm^{-1}).

Construction, Production, and Purification of the PlnE and PlnF Fusion Polypeptides. Synthetic genes (from GenScript) encoding PlnE or PlnF fused to a hexahistidine (His6)-tag, the immunoglobulin-binding domain of streptococcal protein G (GB1-domain; 56 aa), and a nonhelical linker of five consecutive Gly residues between the GB1-domain and the sequence encoding either of the two peptides were cloned into the *Nde*I and *Bam*HI sites of pET-22b(+). The fusion polypeptides were designed in such a way that the fusion-partner was either fused to the N- or C-terminus of the peptides. This resulted in four different vectors. Cloning into pET-22b(+) was performed by GenScript.

The vectors were introduced into competent *E. coli* BL21 (DE3) cells from Invitrogen. Expression of the fusion polypeptides was induced with 1 mM isopropyl β-D-1-thiogalactopyranoside (IPTG) when the OD_{600} of the cell culture had reached approximately 1. The culture was then grown overnight at 250 rpm and 25 °C. Approximately 20 g of cells were harvested by centrifugation, frozen, and lysed using an X-press.[34] The lysed cells were dissolved in 100 mL of 50 mM phosphate buffer, pH 7.4, containing a cocktail of protease inhibitors (cOmplete ULTRA Tablets, EDTA-free; Roche). DNA was removed from the solution with 2% streptomycin sulfate, and the proteins were precipitated with ammonium sulfate (0.33 g/L). The pellet was dissolved in 20 mM phosphate buffer, pH 7.4, and desalted using a 5 mL Hi Trap Desalting column (GE Healthcare) using the ÄKTA chromatography system (GE Healthcare). NaCl and imidazole were added to the eluate to final concentrations of 0.5 M and 20 mM, respectively. The solution was applied to a 5 mL HisTrap HP column (GE Healthcare) equilibrated with 20 mM phosphate buffer (pH 7.4), 0.5 M NaCl, and 20 mM imidazole. The fusion polypeptides were eluted using a linear gradient of 20 mM phosphate buffer, pH 7.4, 0.5 M NaCl, and 0.5 M imidazole. Buffer exchange to 50 mM phosphate buffer, pH 7.4, and concentration of the fusion polypeptides were performed using Amicon Ultra-15 Centrifugal Filter Units with a molecular mass cutoff at 3 kDa (Millipore), at 4 °C. The correct molecular masses of the fusion polypeptides were confirmed by mass spectrometry at the Proteomics Facility at the Department of Biosciences, University of Oslo. The fusion polypeptides were digested with trypsin, and the resulting peptide fragments were analyzed by high performance liquid chromatography-tandem mass spectrometry (HPLC-MS/MS).

The concentration of the fusion polypeptides were determined by UV absorption at 280 nm and calculated using molar extinction coefficients based on the Trp and Tyr residues. The extinction coefficients for the PlnE and PlnF fusion polypeptides were calculated to be 11 560 M^{-1} cm^{-1} and 18 320 M^{-1} cm^{-1}, respectively.

Bacteriocin Activity Assay. For detection of antimicrobial activity of the wild type and mutant variants of PlnE and PlnF

DOI: 10.1021/acs.biochem.6b00588
Biochemistry 2016, 55, 5106−5116

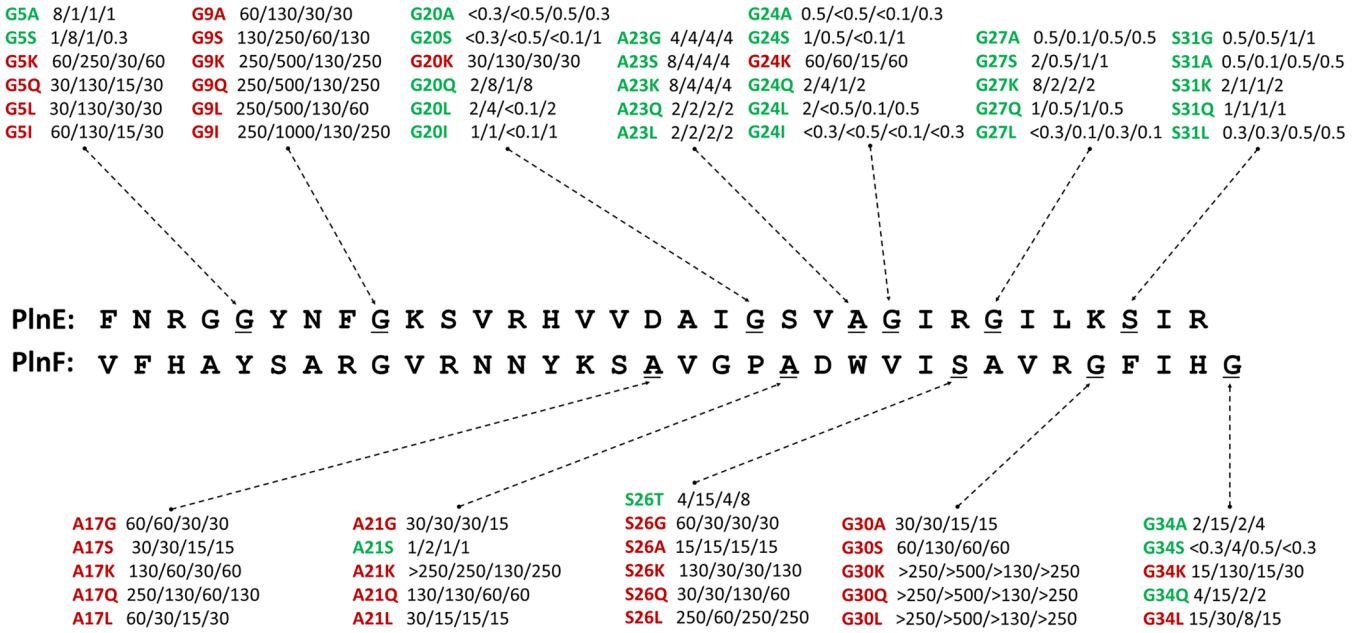

Figure 1. Relative MIC values from activity measurements of four independent parallels of GxxxG and GxxxG-like mutant peptides together with the wild type complementary peptide against the indicator strain *L. curvatus* LTH 1174. The activity is as good as or better than the wild type peptide combination when the number is equal to or less than 1, respectively. Green illustrates mutant peptides with low or no reduction in activity compared to the wild type bacteriocin. Red illustrates peptides where the mutation had a highly detrimental effect on activity (a value of, e.g., 30 means a 30-fold reduction in activity).

as well as the fusion polypeptides, a microtiter plate assay system was used, essentially as described by Nissen-Meyer et al.[35] Each well of the microtiter plate contained MRS medium to a final volume of 200 μL, combinations of wild type and mutated variants of PlnE and PlnF (in 1:1 ratio), and one of the four indicator strains. The fusion polypeptides were added at a 10:1 molar ratio with respect to the concentration of the complementary wild type peptide. The dilution factor of the peptide combinations was 2-fold going from one well to the next. Stationary phase cultures of indicator strains were diluted 1:50 and the microtiter plates were incubated for 5 h at 30 °C. The growth of the indicator cells was measured spectrophotometrically at 600 nm by use of a Sunrise Remote microplate reader (Tecan).

The minimum inhibitory concentration (MIC) was defined as the total amount of wild type or peptide mutants of PlnE and PlnF, at a 1:1 ratio, that inhibited the growth of the indicator strain by 50%. The relative MIC value was quantitated in terms of fold increase or decrease in activity compared to the wild type combination.

Building the Dimer Model. The structure of the dimer was calculated using CYANA,[36] and the structural restraints for PlnE (PDB ID code: 2jui) and PlnF (PDB ID code: 2rlw) were downloaded from the protein data bank. In addition to these, distance restraints were inserted between residues in the GxxxG-like motifs; PlnE G5 CA and HA2 to PlnF G30 O, and PlnE G9 CA and HA2 to PlnF S26 O, the upper distances were 2.7 and 3.7 Å, respectively.[37] We also added upper distance structure restraints of 3 Å between PlnE R13 NH1 and NH2 and PlnF D22 OD1 and OD2, and between PlnE D17 OD1 and OD2 to PlnF K15 NZ. 100 structures were calculated and the lowest energy structure was used as a dimer model in the molecular dynamics simulations.

Molecular Dynamics (MD) Simulation Methods and Parameters. The dimer was placed into the model membrane using the online server CHARMM-GUI.[38] Two distinct models were built by positioning the dimer at different distances from the center of the membrane along the *z* axis. In model one, the dimer was placed with the aromatic residues on the surface of the lower leaflet and the peptides penetrating through both the upper and lower surface of the model membrane. In model two, the residues W23 of PlnF and Y6 of PlnE lie inside the membrane core.

The lipid bilayer was built to mimic the membrane of Gram-positive bacteria, using 1-palmitoyl-2-oleoyl-*sn*-glycero-3-phosphoglycerol (POPG) and 1-palmitoyl-2-oleoyl-*sn*-glycero-3-phosphoethanolamine (POPE) lipids in a 3:1 ratio.[17,24] The dimer−membrane systems were solvated in a 0.15 M NaCl aqueous solution with the VMD software.[39] Counterions were added as necessary to electroneutralize each system.

NAMD 2.10[40] was used for molecular dynamics simulations, with the CHARMM param36 force field.[41] Systems were first minimized with a conjugate gradient algorithm and then gradually heated to 310 K. Equilibration and production runs were carried out at constant temperature and atmospheric pressure, using the Nose-Hover algorithm provided in NAMD.

Simulations were conducted for 200 ns using a 2 fs time step. The van der Waals potential was turned off at 12 Å, introducing a switching function at 10 Å. Electrostatic interactions were calculated with the particle mess Ewald summation, with a real space cutoff truncated at 12 Å.

RESULTS AND DISCUSSION

Mutational Effects on the GxxxG and GxxxG-like Motifs. To determine whether the GxxxG and GxxxG-like motifs might be involved in helix−helix interactions between PlnE and PlnF, the glycine, alanine, and serine residues in these motifs were replaced with other small residues (Ala, Gly, Ser) and with large hydrophobic (Ile and/or Leu) and hydrophilic (Gln, Lys) residues. The activity of the various peptide variants,

DOI: 10.1021/acs.biochem.6b00588
Biochemistry 2016, 55, 5106−5116

together with the complementary wild type peptide, was assayed against four different indicator strains (*L. viridescens* NCDO 1655, *P. pentosaceus* NCDO 990, *P. acidilatici* NCDO 521, and *L. curvatus* LTH 1174). Four indicator strains were chosen because activity related to mutational effects may in some cases be strain-dependent.[42−44] In total, 39 and 26 mutated variants of PlnE and PlnF, respectively, were assayed against the four indicator strains. The activity of the mutated peptide variants in combination with the complementary wild type peptide was compared with the wild type combination, and the results are represented as relative MIC values in Figure 1. The results presented in Figure 1 are based on the activity tested against *L. curvatus* LTH1174; the strain is about 10 times more sensitive to wild type plantaricin EF than the three other indicator strains. Overall, the relative MIC values for all four strains were comparable, but the effects of mutations on relative MIC values are overall greater when using *L. curvatus* LTH1174 because of its higher sensitivity to wild type plantaricin EF (see Table S2 in Supporting Information).

The GxxxG and GxxxG-like Motifs in PlnE. The effect the mutations had on the antimicrobial activity varied considerably between the two GxxxG motifs in PlnE; nearly all replacements of the glycine residues in the G_5xxxG_9 motif were detrimental, while nearly all similar replacements in the $G_{20}xxxG_{24}$ motif were tolerated. The only mutations that were tolerated in the G_5xxxG_9 motif were the G5A and G5S mutations, as almost all activity was retained with these replacements (Figure 1). In contrast, replacing this glycine residue with large hydrophilic (G5K and G5Q) or hydrophobic (G5I and G5L) residues reduced the activity 10−200 fold (Figure 1). Replacement of the other glycine residue, Gly9, in the G_5xxxG_9 motif was not tolerated at all. Even replacements with small residues (G9A and G9S) caused a 30−200 fold reduction in the activity, while replacements with large hydrophilic (G9Q and G9K) or hydrophobic (G9I and G9L) residues reduced the activity 100−1000 fold (Figure 1). This indicates that these two Gly residues are in a structurally restricted environment, possibly needed for close interhelical contact with the complementary peptide. In sharp contrast, the glycine residues in the $G_{20}xxxG_{24}$ motif in PlnE tolerated nearly all substituents quite well. Individual replacements of these glycine residues with small (Ala and Ser) and large hydrophobic (Ile and Leu) and hydrophilic (Gln) residues resulted in similar or somewhat higher activity than the wild type combination (Figure 1). Introducing a positive charge at positions 20 and 24 was, however, detrimental. The G20K and G24K mutations resulted in approximately a 50 fold reduction in activity (Figure 1). These results indicate that Gly20 and Gly24 (in contrast to Gly5 and Gly9) are not in a structurally restricted environment, nor in a strictly hydrophobic or hydrophilic environment, and that the $G_{20}xxxG_{24}$ region is not in close interhelical contact with the complementary peptide. The same tendency is also seen for the two GxxxG-like motifs, $A_{23}xxxG_{27}$ and $G_{27}xxxS_{31}$. Substituting the small residues with other amino acids such as small, large hydrophilic or large hydrophobic residues did not seem to greatly affect the antimicrobial activity (Figure 1).

The GxxxG and GxxxG-like Motifs in PlnF. Except for the A21S mutation, which was well tolerated, all replacements of the two alanine residues in the GxxxG-like motif $A_{17}xxxA_{21}$ in PlnF were detrimental. Even replacements with a small glycine residue were detrimental, as the A17G and A21G mutations reduced the activity 30−60 and 15−30 fold, respectively (Figure 1). Notably, replacing these alanine residues with a large hydrophobic residue (Leu) was somewhat less detrimental than replacement with a glycine residue, as the A17L and A21L mutations reduced the activity only 10−30 fold (Figure 1). Replacements with a large hydrophilic residue were more detrimental than replacement with a leucine residue, as the A17K and A21Q mutations reduced the activity 30−60 fold and the A17Q and A21K mutations reduced the activity 60−130 fold (Figure 1). The fact that replacements with leucine residues were less detrimental than replacements with glycine residues indicates that the $A_{17}xxxA_{21}$ region is not in close interhelical contact with the complementary peptide. However, the detrimental effect of the glycine substitutions does indicate that the increased flexibility induced in the helix is nonbeneficial for the function of the bacteriocin; thus the helix in this region of the peptide is important for function.

The OH-group in Ser26, which is part of the GxxxG-like motif $S_{26}xxxG_{30}$, is apparently involved in hydrogen bonding, since replacement with a threonine residue—which also contains an OH-group—resulted in only a 4−15-fold reduction in the activity and was the substitution that was best tolerated (Figure 1). Replacement of Ser26 with a glycine or alanine residue reduced the activity about 15−30 fold, while replacement with a large hydrophilic (Lys and Gln) or a large hydrophobic residue (Leu) caused, respectively, a 30−130 fold and 60−250 fold reduction in the activity (Figure 1). A small residue with hydrogen bonding properties seems to be preferred in position 26.

All the replacements of Gly30, which is in both the $S_{26}xxxG_{30}$ and $G_{30}xxxG_{34}$ motifs, were detrimental, indicating that Gly30 is in a structurally restricted environment. Substituting Gly30 with small residues such as Ala and Ser were the least detrimental replacements, causing a 15−30 and 60−130 fold reduction in activity, respectively (Figure 1). The other mutations, G30K, G30Q, and G30L were highly detrimental, causing more than a 500 fold reduction in the activity (Figure 1). The other glycine residue, Gly34, in the $G_{30}xxxG_{34}$ motif was, however, less restricted, as replacement with Ser resulted in wild type or better than wild type activity, and replacement with Ala and the larger hydrophilic Gln residue reduced the activity 2−15-fold (Figure 1). Replacement with a hydrophobic leucine residue (G34L) and a hydrophilic charged lysine residue (G34K) reduced the activity, respectively, 10−30 and 15−130 fold (Figure 1). The greater flexibility of Gly34 in PlnF compared to Ser26 and Gly30 in PlnF and Gly5 and Gly9 in PlnE is possibly due to the fact that Gly34 is the last residue in PlnF, and this enables the residue to fluctuate to a greater extent than internal residues. The highly restricted environment of Gly30 suggests that Gly30, as part of the $S_{26}xxxG_{30}$ or $G_{30}xxxG_{34}$ motif in PlnF, might be in close interhelical contact—in either a parallel or antiparallel orientation—with the G_5xxxG_9 motif in PlnE.

Orientation of Plantaricin EF in Target-Cell Membranes. In order to determine the orientation of PlnE and PlnF in target-cell membranes and whether the two peptides interact in a parallel or antiparallel manner, we constructed four fusion polypeptides in which the hydrophilic GB1-domain was fused to either the N- or C-terminal ends of PlnE and PlnF. The two fusion polypeptides in which the GB1-domain is attached to the ends of the Pln-peptides that enter into or traverse the target-cell membrane are expected to be inactive. In contrast, the two fusion polypeptides in which the GB1-domain is attached to the ends of the Pln-peptides that do not enter into the hydrophobic part of the membrane may still have some

DOI: 10.1021/acs.biochem.6b00588
Biochemistry 2016, 55, 5106−5116

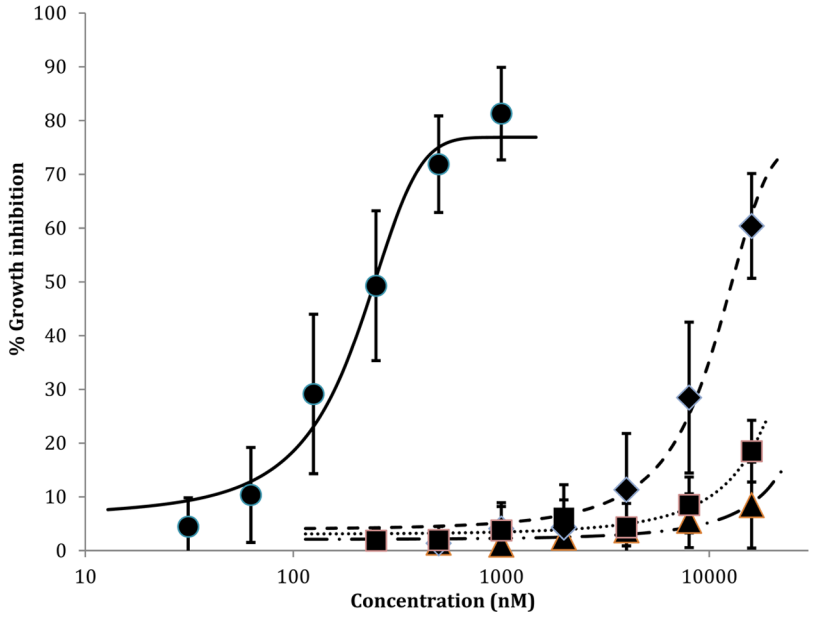

Figure 2. Activity measurements of the four fusion polypeptides. The *y*-axis represents % growth inhibition of *L. curvatus* LTH1174 based on the OD_{600} in microtiter plate assays and the *x*-axis represents the nanomolar concentration as a $\log_{10}$ scale of the respective fusion polypeptides. The concentration of the complementary wild type peptide PlnF was added at a concentration of 4000 nM in the first well of the microtiter plate assay together with either C-PlnE or N-PlnE, whereas the wild type PlnE peptide was added at a concentration of 400 nM (combined with either C-PlnF or N-PlnF). The error bars represent the ± standard deviations from at least three independent measurements. Circles represents C-PlnE, diamonds N-PlnF, squares C-PlnF, and triangles N-PlnE.

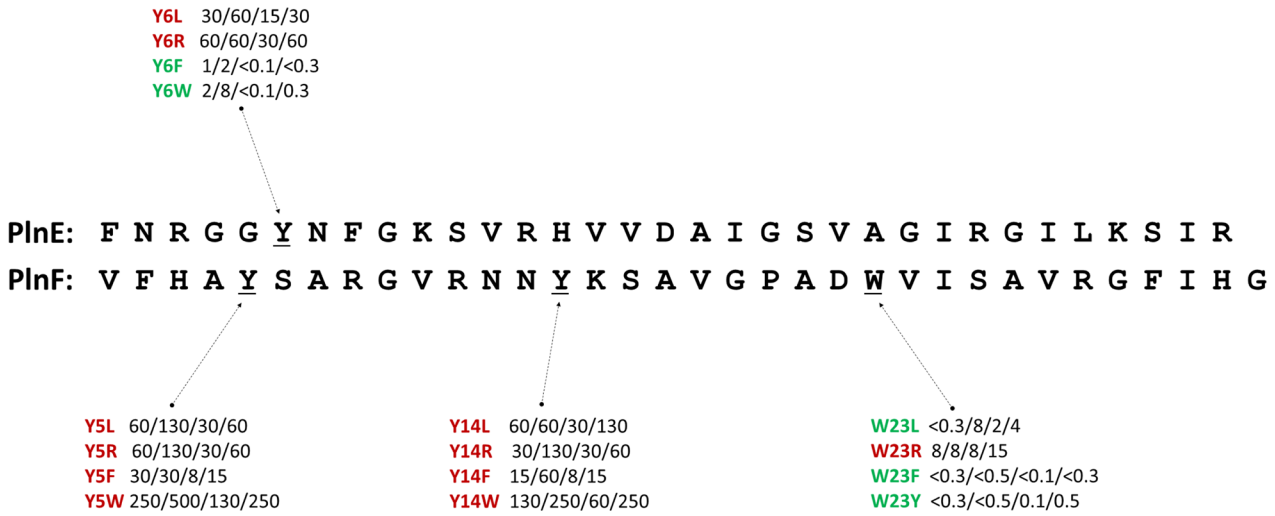

Figure 3. Relative MIC values from activity measurements of aromatic mutant peptides complemented with the wild type peptide against the indicator strain *L. curvatus* LTH1174. The activity is as good as or better than the wild type peptide combination when the number is equal to or less than 1, respectively. Green illustrates mutant peptides with low or no reduction in activity compared to the wild type bacteriocin. Red illustrates peptides where the mutation had a highly detrimental effect on antimicrobial activity.

antimicrobial activity. The activity may, however, be greatly reduced compared to the wild type peptides due to possible steric interference by the GB1-domain. The penta-Gly linker between the GB1-domain and the Pln-peptides was included in order to increase the structural flexibility and thus reduce steric obstructions. The indicator strain, *L. curvatus* LTH 1174, that is most sensitive to plantaricin EF was used when assaying the activity of the four fusion polypeptides. A similar approach has earlier been successfully used to study the orientation in membranes of the class-IIa bacteriocin pediocin PA-1[45] and the class IIb bacteriocin lactococcin G.[10]

The four fusion polypeptides were named according to the side of the peptide to which the GB1-domain was attached; for N-PlnE and N-PlnF the GB1-domain is attached at the N-terminus of PlnE and PlnF, respectively, and for C-PlnE and C-PlnF the GB1-domain is attached at their C-termini (see Figure S1 in the Supporting Information for the amino acid sequence of the four fusion polypeptides). Before assaying the purified fusion polypeptides for bacteriocin activity, a trypsin digested sample of each polypeptide was analyzed by mass spectrometry. The correct N- and C-terminal fragments were identified (along with the other major internal fragments) for all four polypeptides (results not shown), thus confirming that intact

DOI: 10.1021/acs.biochem.6b00588
Biochemistry 2016, 55, 5106−5116

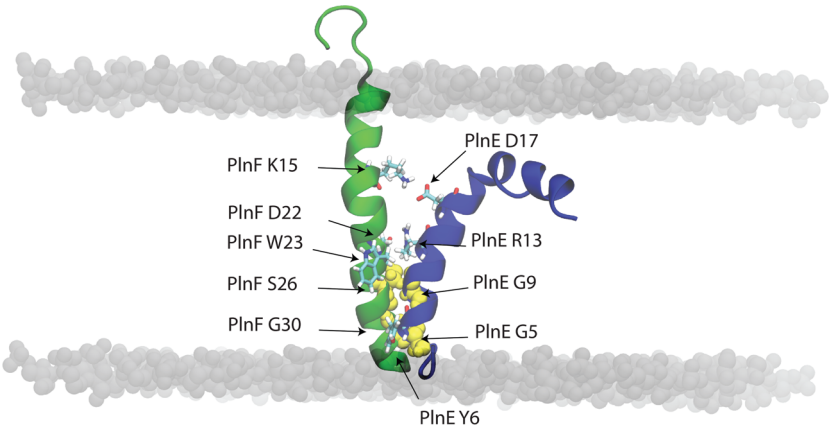

Figure 4. Model of the plantaricin EF dimer resulting from combining the structural restraints from the structure determination of the individual peptides in dodecylphosphocholine (DPC) micelles and the results from activity assays on mutants of PlnE and PlnF. PlnF is shown in green, while PlnE is shown in blue. The headgroup atoms of the lipids are shown as gray spheres. Glycine and serine residues thought to be important for the interaction between the two peptides are drawn as yellow spheres. Other important residues are drawn in stick representation. See the text for further details.

fusion polypeptides were used when assaying for bacteriocin activity.

When applied together with the complementary wild type peptide, PlnF, the C-PlnE fusion polypeptide displayed bacteriocin activity at 0.2 μM concentrations and higher, whereas the N-PlnE fusion polypeptide showed no significant activity even at concentrations up to 20 μM (Figure 2). The N-PlnF fusion polypeptide together with its complementary wild type peptide, PlnE, displayed bacteriocin activity at 10 μM concentrations and higher, whereas the C-PlnF fusion polypeptide showed no significant activity at concentrations up to 20 μM (Figure 2). These results indicate that the C-terminus of PlnE and the N-terminus of PlnF are located on the outer part of the target-cell membrane, and that the two peptides thus interact in an antiparallel manner when integrated in the membrane. The two active fusion polypeptides, C-PlnE and N-PlnF, resulted in greatly reduced activity compared to the wild type peptides; whereas the latter display activity at nanomolar concentrations, the former were only active at concentrations in the micromolar range. In view of the possibility for steric interactions between the GB1-domain and either the membrane or the receptor this result is not unexpected.

Effects of Aromatic Substitutions. It is known that the aromatic residues Tyr and especially Trp prefer to position themselves in the membrane interface and may therefore be important contributors to the anchoring of the peptides in the membrane.[42,46−49] To test the role of these residues, Trp and Tyr were substituted with either a large hydrophobic residue (Leu), a large, positively charged residue (Arg), the hydrophobic aromatic residue Phe as well as either Trp or Tyr. Replacement of Tyr at position 6 in PlnE with a Leu or Arg (Y6L and Y6R) resulted in a 15−60 fold reduction in activity (Figure 3). All activity was retained when substituting Tyr with the aromatic residues Phe and Trp (Y6F and Y6W). The preference for an aromatic residue at this location in PlnE indicates a positioning in the membrane interface, possibly on the inner part of the membrane, since the results obtained with the fusion polypeptides suggest that the C-terminus of PlnE is on the outer part of the membrane. Substituting the two Tyr residues in PlnF at positions 5 and 14 with either a Leu or an Arg reduced the activity 30−130 fold, whereas replacing it with Phe caused a 10−50 fold reduction in activity (Figure 3). Replacing these Tyr residues with a Trp, however, was very detrimental on the activity, reducing it 100− 300 fold, implicating a spatial restriction on these sites and possibly also hydrogen bonding opportunities mediated by the OH-group of Tyr. The Trp residue at position 23 in PlnF did not seem to have any specific preferences for an aromatic side chain since replacing it with either Leu, Phe, or Tyr resulted in equal or better than wild type activity. The positively charged Arg residue (W23R) resulted in 8−15-fold decrease in activity, suggesting a preference for hydrophobicity and a possible positioning in or near the hydrophobic core of the membrane.

Model of Plantaricin EF Inserted into Membrane Bilayer Based on Mutational Assays and the Known NMR Structures of the Individual Peptides. The results presented above indicate that PlnE and PlnF interact in an antiparallel manner and that the G_5xxxG_9 motif in PlnE and the $S_{26}xxxG_{30}$ or $G_{30}xxxG_{34}$ motifs PlnF are involved in helix−helix interactions. However, due to Gly34 being the last residue in PlnF, the $G_{30}xxxG_{34}$ motif is an unlikely candidate for helix−helix stabilization. More importantly, an antiparallel interaction between $G_{30}xxxG_{34}$ in PlnF and G_5xxxG_9 in PlnE results in strong charge repulsion between the peptides. The positively charged residues Arg13 in PlnE and Arg29 in PlnF come close in space when the peptides are arranged using these GxxxG motifs. This is also the case for the negatively charged Asp17 in PlnE and Asp22 in PlnF. Moreover, previous MD simulation of the two Pln-peptides revealed that the G_5xxxG_9 motif in PlnE and the $G_{30}xxxG_{34}$ motif PlnF did not bring the two peptides in close contact; the peptides interacted only weakly—only one salt bridge (between Arg13 in PlnE and Asp22 in PlnF) was formed—and the potential energy of interaction between the peptides was positive.[17]

The other possibility, that G_5xxxG_9 in PlnE and $S_{26}xxxG_{30}$ in PlnF interact in an antiparallel manner, results in a dimer that may be stabilized by two salt bridges between Arg13 in PlnE and Asp22 in PlnF and between Asp17 in PlnE and Lys15 in PlnF. This conformation is consistent with the observation that changing the charges of these residues was detrimental to the antimicrobial activity.[17] Figure 4 represents a structural model of plantaricin EF in which the two peptides interact through the G_5xxxG_9 motif in PlnE and the $S_{26}xxxG_{30}$ motif in PlnF in an

DOI: 10.1021/acs.biochem.6b00588
Biochemistry 2016, 55, 5106−5116

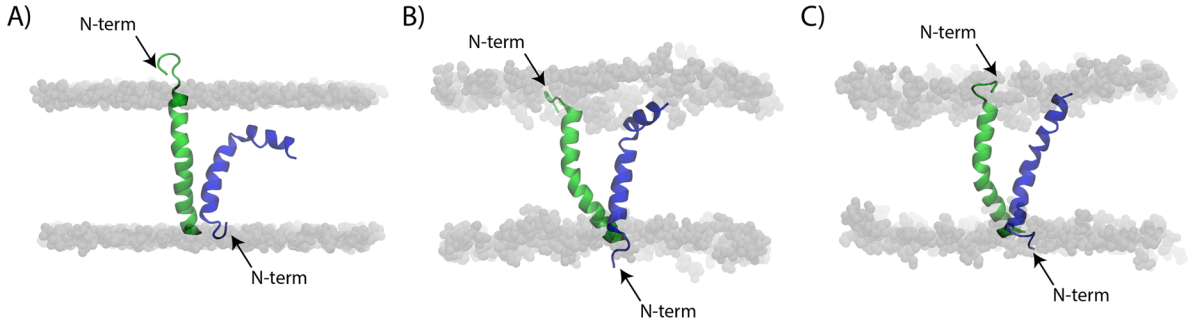

Figure 5. Plantaricin EF dimer model at different time steps during the molecular dynamics simulation. The figures at 0 ns, 50 and 200 ns are shown in panels A, B, and C, respectively. PlnF is shown in a green cartoon drawing in all the pictures, while PlnE is shown in blue. The headgroup atoms of the lipids are shown as gray spheres.

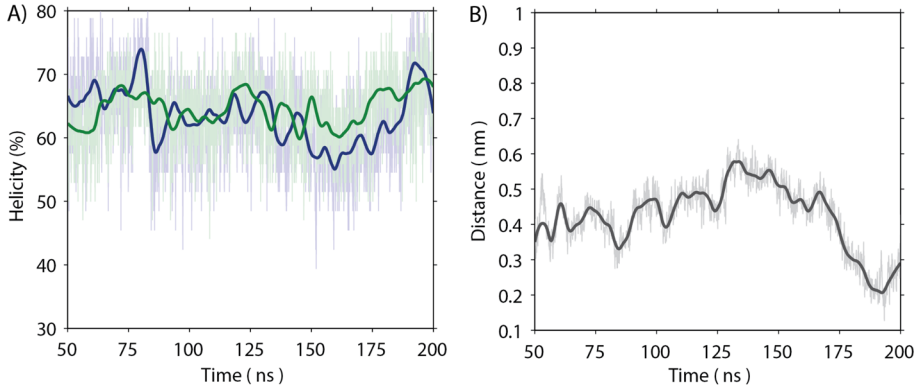

Figure 6. Molecular dynamics simulation trajectories between 50 and 200 ns. In (A) the α-helicity of PlnE is shown in % in blue, and the PlnF in green. Distance between the center of mass of PlnE G5 and G9 and center of mass of PlnF S26 and G30 motifs are shown in (B). Thin lines illustrate the measured distances in each frame, while the thick lines illustrate the sliding average.

antiparallel transmembrane orientation in a model lipid bilayer. In this structural model, the N-terminus of PlnE and C-terminus of PlnF form a blunt end. In contrast, there is a one amino acid overhang on PlnF in the other end, formed by the C-terminus of PlnE and N-terminus of PlnF, both of which (according to the results obtained with the fusion polypeptides) face toward the cell's outside (Figure 4). The preference for an aromatic residue at position 6 in PlnE, Tyr6, suggests that this end positions itself in or near the membrane interface on the cytosolic side of the membrane. In this model, residues Arg8, Arg11, and Lys15 in PlnF are brought close to PlnE Gly20 and Gly24 and may explain the detrimental effect of substituting the latter two residues with the positively charged Lys, while being able to accommodate all other substitutions (Figure 1).

Molecular Dynamics (MD) Simulation and Evaluation of the Membrane-Inserted Model of Plantaricin EF. To evaluate the results, a model fitting the above-mentioned criteria was inserted into a lipid bilayer and analyzed using MD simulation. In this simulation, only very small changes were observed in the structure and orientation during the 200 ns of MD simulation as can be seen in Figures 5, 6, and 7. Both peptides are mostly helical during the last 150 ns of simulation (Figure 6A).

The distance between the G_5xxxG_9 motif in PlnE and $S_{26}xxxG_{30}$ motif in PlnF seems to be fairly stable and even decreases toward the end of the MD simulation (Figure 6B), indicating that the overall interaction around the suggested interaction motifs improves during the simulation. Several interactions between the peptides seem to be of importance during the simulation. Importantly, we observe the same intermolecular hydrogen bonds/salt bridges as hypothesized, that is, between PlnE R13 and PlnF D22 and to a lesser extent between PlnE D17 and PlnF K15 as illustrated in Figures 7A,B and S2. Interestingly, K15 seems to switch interaction partners, between PlnE D17 and PlnF N12, back and forth throughout the simulation, the latter residue being closer to the outer lipid head groups (Figure S5). In addition, besides the strong electrostatic interaction, there is also an intramolecular hydrogen bond between PlnE D17 and PlnE R13 (Figure S3A), further stabilizing the "polar center" of the dimer. The combination of hydrogen bonds between PlnE D17, PlnE R13, and PlnF D22 that are present throughout the simulation may in fact be a variation of a cluster of interhelical hydrogen bonds/salt bridges called "polar clamps", which is a common motif found in the transmembrane regions of membrane proteins.[50] There is also a hydrogen bond between PlnE R3 and the terminal oxygen at the C-terminal of PlnF on G34 during most of the simulation (Figure S2).

The MD analysis also reveals that the dimer is further stabilized by aromatic interactions and cation-π interactions. Consistent with the results from the mutation studies, the aromatic amino acid Tyr at position 6 in PlnE seems to be stably inserted into the inner membrane interface of the lipid bilayer (Figure 7C,D). Furthermore, this residue interacts via a staggered (parallel) cation-π interaction with the aromatic residue F31 in PlnF. A T-shaped cation-π interaction is observed for PlnF W23 and H14 in PlnE as well. In fact, W23 seems to coordinate with both PlnE H14 and PlnE K10 in such a way that if one of these residues changed slightly in position, the others moved as well, keeping a stable internal distance

DOI: 10.1021/acs.biochem.6b00588
Biochemistry 2016, 55, 5106−5116

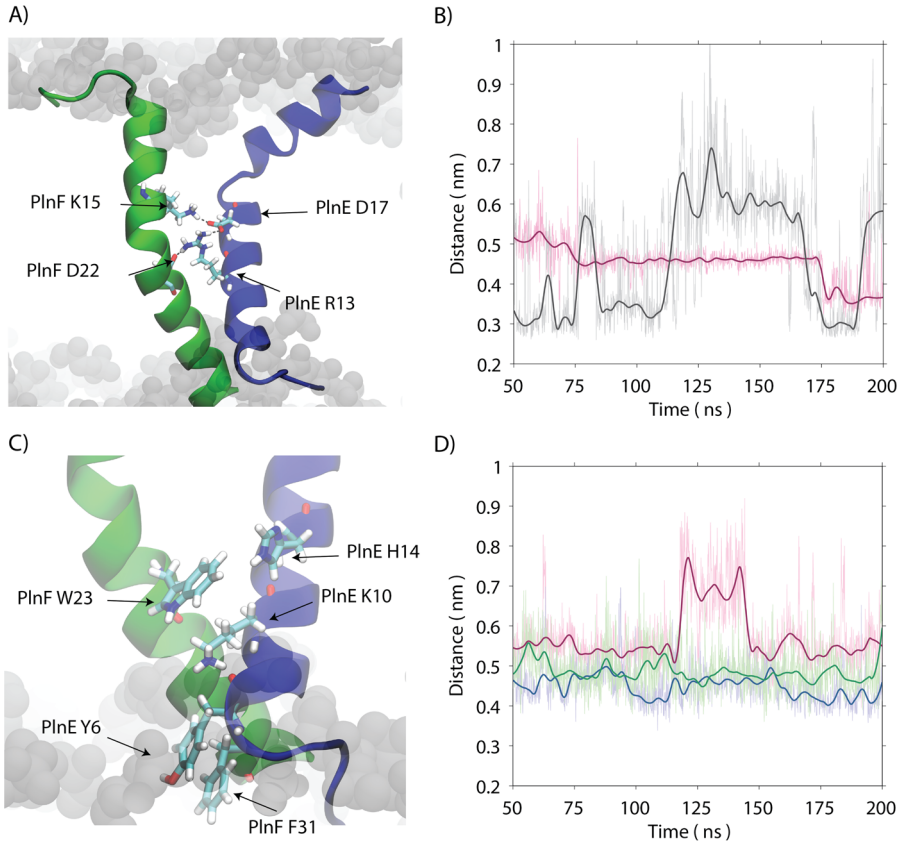

Figure 7. Molecular structures at the end of the molecular dynamics simulation and trajectories of interactions important for stabilization of plantaricin EF. The important residues stabilizing the two peptides are shown in (A) and (C), while trajectories showing the variation in distances in the MD simulations between 50 and 200 ns are shown in (B) and (D). In (A) and (B) the stabilizing electrostatic interactions are shown, while the aromatic ring stacking and lysine contributing to cation-π interactions are shown in (C) and (D). The structures depicted in (A) and (C) are in the cartoon drawing, PlnE is in blue and PlnF is in green, and the lipid head groups are shown as gray spheres. Atoms of the residues of importance are colored according to atom type: carbon is in light green, hydrogen is white, oxygen is red, and nitrogen is blue. The curves in (B) and (D) are between the center of mass of the aromatic rings, carboxyl, guanidinium, or ammonium groups. In (B) the red and black curves are between PlnE R13 and PlnF D22 and between PlnE D17 and PlnF K15, respectively. In (D) the red, blue, and green curves are for the distances between PlnE H14 and PlnF W23, PlnE K10 and PlnF W23, and between PlnE Y6 and PlnF F31, respectively. Thin lines in (B) and (D) illustrate the measured distances in each frame, while the thick lines illustrate the sliding average.

throughout the simulation, the only exception being the distance between W23 in PlnF and H14 in PlnE in the time frame between 115−150 ns (Figure 7C,D). The W23−K10 cation-π interaction may help stabilize the dimerization in a similar manner as reported by Peter et al. for the chloride intracellular channel protein 1 transmembrane domain.[51]

S26 in PlnF is initially hydrogen bonded with the backbone carbonyl oxygen of G9 in PlnE the first 100 ns of simulation, before it switches to an intramolecular hydrogen bond with D22 during the final 100 ns (Figures S2, S3, and S4). This is, however, not the only serine in the peptides that is hydrogen bonded. In both PlnE and PlnF there is a pattern of three Ser residues separated by nine other residues. In PlnE, all of these serine hydroxyl groups are hydrogen bonded at least part of the time to the carboxyl group of residues i-4 (Figures S3 and S4). Similar hydrogen bonds are also observed for PlnF between S16 and N12 and S26 and D22 (Figures S3 and S4). These serine interactions may be of importance in internal stabilization of the helices and might explain why Ser instead of Gly is in the $S_{26}xxxG_{30}$ motif in PlnF.

The transmembrane bacteriocin dimer interacts with the lipid phosphate groups through a number of hydrogen bonds (Figure S5). In PlnE, residues R26, K30, and K33 in the C-terminal region and F1, R3, Y6, N7, and K10 in the N-terminal region interact with, respectively, the outer and inner lipid phosphate groups. PlnF anchors to both the inner and outer lipid phosphate groups through its C-terminal residues R29, H33, and G34 and N-terminal residues V1, F2, H3, Y5, S6, A7, R8, R11, N12, N13, Y14, and K15, respectively (Figure S5). The hydrogen bonds formed between hydroxyl groups of PlnF Y5 and PlnF Y14 with the lipid phosphate groups may to some extent explain why substituting with hydrophobic, positively charged, or aromatic amino acids was detrimental to activity.

To determine whether the stability of the plantaricin EF structure shown in Figure 4 depends on it being in a transmembrane position and in a predominantly hydrophobic environment, we also performed a simulation in which the structure was partly inserted into the membrane (instead of as a transmembrane entity; Figure S6). In this latter simulation, the structure is also in agreement with the results above except that Tyr6 in PlnE is no longer in the membrane interface, but rather in the hydrophobic core of the membrane. After approximately 50 ns, the peptides moved toward the membrane surface and ended up positioned on the surface of the bilayer (Figure S6), perhaps not unexpected, since substituting Tyr6 with a hydrophobic amino acid was detrimental to the bacteriocin

DOI: 10.1021/acs.biochem.6b00588
Biochemistry 2016, 55, 5106−5116

activity. Furthermore, the bacteriocin structure lost much of its α-helical character—and therefore becomes inconsistent with the NMR structures[14]—during the MD simulation (Figure S7). The results are thus consistent with the insertion of plantaricin EF in a transmembrane orientation.

In summary, the MD simulations confirmed the stability of the structure and its orientation in the membrane as shown in Figure 4 by approving the interactions anticipated from the mutational studies. The MD simulations also revealed additional interactions that further increase the stability of the dimer and explained some detrimental mutations, such as PlnE G20K and G24K.

■ ASSOCIATED CONTENT

Supporting Information

The Supporting Information is available free of charge on the ACS Publications website at DOI: 10.1021/acs.biochem.6b00588.

Additional experimental details; relative MIC values of all mutated peptide variants tested against four indicator strains; amino acid sequence of the four fusion polypeptides; inter- and intramolecular interactions between PlnE and PlnF; interactions between the serine residues in PlnE and PlnF during MD simulation; hydrogen bonds between the Pln-peptides and the membrane; alternative plantaricin EF dimer model (PDF)

■ AUTHOR INFORMATION

Corresponding Authors

*(B.E.) E-mail: bie.ekblad@ibv.uio.no.

*(P.E.K.) E-mail: p.e.kristiansen@ibv.uio.no.

Funding

This project was funded partially by the Norwegian Centennial Chair program, a cooperation in research and academic education between the Norwegian University of Life Science, the University of Oslo and the University of Minnesota and partially by a grant from the U.S. National Institutes of Health (GM111358). B.E. has been funded by the Molecular Life Science initiative at the University of Oslo. Part of this work utilized the high-performance computational resources of the Extreme Science and Engineering Discovery Environment (XSEDE), which is supported by National Science Foundation Grant Number ACI-1053575.

Notes

The authors declare no competing financial interest.

■ ACKNOWLEDGMENTS

Computational support from the Minnesota Supercomputing Institute (MSI) is gratefully acknowledged. We thank Benedicte M. Jørgenrud for constructing the plasmid pPlnF100 and for creating some of the plasmids resulting in mutated variants of PlnF.

■ ABBREVIATIONS

AMPs, antimicrobial peptides; CD, circular dichroism; DPC, dodecylphosphocholine; GB1-domain, immunoglobulin-binding domain of streptococcal protein G; GRAS, generally recognized as safe; HPLC, high performance liquid chromatography; IPTG, isopropyl β-D-1-thiogalactopyranoside; LAB, lactic acid bacteria; LB, lysogeny broth; MALDI-TOF, matrix-assisted laser desorption/ionization-time-of-flight; MD, molecular dynamics; MIC, minimum inhibitory concentration; MRS, de Man-Rogosa-Sharpe; MS, mass spectrometry; NMR, nuclear magnetic resonance; OD_{600}, optical density at 600 nm; PCR, polymerase chain reaction; PCRSOEing, polymerase chain reaction - splicing by overlap extension; PlnE, plantaricin E; PlnF, plantaricin F; PlnI, plantaricin I; POPG, 1-palmitoyl-2-oleoyl-*sn*-glycero-3-phosphoglycerol; POPE, 1-palmitoyl-2-oleoyl-*sn*-glycero-3-phosphoethanolamine; TFA, trifluoroacetic acid

■ REFERENCES

(1) Hancock, R. E. W., and Diamond, G. (2000) The role of cationic antimicrobial peptides in innate host defences. *Trends Microbiol. 8*, 402−410.

(2) Nissen-Meyer, J., and Nes, I. F. (1997) Ribosomally synthesized antimicrobial peptides: Their function, structure, biogenesis, and mechanism of action. *Arch. Microbiol. 167*, 67−77.

(3) Nissen-Meyer, J., Rogne, P., Oppegård, C., Haugen, H. S., and Kristiansen, P. E. (2009) Structure-function relationships of the non-lanthionine-containing peptide (class II) bacteriocins produced by gram-positive bacteria. *Curr. Pharm. Biotechnol. 10*, 19−37.

(4) Cotter, P. D., Hill, C., and Ross, R. P. (2005) Bacteriocins: developing innate immunity for food. *Nat. Rev. Microbiol. 3*, 777−788.

(5) Anderssen, E. L., Diep, D. B., Nes, I. F., Eijsink, V. G. H., and Nissen-Meyer, J. (1998) Antagonistic activity of *Lactobacillus plantarum* C11: Two new two-peptide bacteriocins, plantaricins EF and JK, and the induction factor plantaricin A. *Appl. Environ. Microbiol. 64*, 2269−2272.

(6) Hauge, H. H., Mantzilas, D., Eijsink, V. G., and Nissen-Meyer, J. (1999) Membrane-mimicking entities induce structuring of the two-peptide bacteriocins plantaricin E/F and plantaricin J/K. *J. Bacteriol. 181*, 740−747.

(7) Diep, D. B., Håvarstein, L. S., and Nes, I. F. (1996) Characterization of the locus responsible for the bacteriocin production in *Lactobacillus plantarum* C11. *J. Bacteriol. 178*, 4472−4483.

(8) Moll, G. N., van den Akker, E., Hauge, H. H., Nissen-Meyer, J., Nes, I. F., Konings, W. N., and Driessen, A. J. M. (1999) Complementary and overlapping selectivity of the two-peptide bacteriocins plantaricin EF and JK. *J. Bacteriol. 181*, 4848−4852.

(9) Zhang, X., Wang, Y., Liu, L., Wei, Y., Shang, N., Zhang, X., and Li, P. (2016) Two-peptide bacteriocin PlnEF causes cell membrane damage to *Lactobacillus plantarum*. *Biochim. Biophys. Acta, Biomembr. 1858*, 274−280.

(10) Oppegård, C., Rogne, P., Emanuelsen, L., Kristiansen, P. E., Fimland, G., and Nissen-Meyer, J. (2007) The two-peptide class II bacteriocins: structure, production, and mode of action. *J. Mol. Microbiol. Biotechnol. 13*, 210−219.

(11) Kjos, M., Oppegård, C., Diep, D. B., Nes, I. F., Veening, J. W., Nissen-Meyer, J., and Kristensen, T. (2014) Sensitivity to the two-peptide bacteriocin lactococcin G is dependent on UppP, an enzyme involved in cell-wall synthesis. *Mol. Microbiol. 92*, 1177−1187.

(12) Oppegård, C., Kjos, M., Veening, J. W., Nissen-Meyer, J., and Kristensen, T. (2016) A putative amino acid transporter determines sensitivity to the two-peptide bacteriocin plantaricin JK. *MicrobiologyOpen 5*, 700.

(13) Hauge, H. H., Nissen-Meyer, J., Nes, I. F., and Eijsink, V. G. (1998) Amphiphilic alpha-helices are important structural motifs in the alpha and beta peptides that constitute the bacteriocin lactococcin G: enhancement of helix formation upon alpha-beta interaction. *Eur. J. Biochem. 251*, 565−572.

(14) Fimland, N., Rogne, P., Fimland, G., Nissen-Meyer, J., and Kristiansen, P. E. (2008) Three-dimensional structure of the two peptides that constitute the two-peptide bacteriocin plantaricin EF. *Biochim. Biophys. Acta, Proteins Proteomics 1784*, 1711−1719.

(15) Rogne, P., Fimland, G., Nissen-Meyer, J., and Kristiansen, P. E. (2008) Three-dimensional structure of the two peptides that

DOI: 10.1021/acs.biochem.6b00588
Biochemistry 2016, 55, 5106−5116

constitute the two-peptide bacteriocin lactococcin G. *Biochim. Biophys. Acta, Proteins Proteomics 1784*, 543−554.
(16) Rogne, P., Haugen, C., Fimland, G., Nissen-Meyer, J., and Kristiansen, P. E. (2009) Three-dimensional structure of the two-peptide bacteriocin plantaricin JK. *Peptides 30*, 1613−1621.
(17) Kyriakou, P. K., Ekblad, B., Kristiansen, P. E., and Kaznessis, Y. N. (2016) Interactions of a class IIb bacteriocin with a model lipid bilayer, investigated through molecular dynamics simulations. *Biochim. Biophys. Acta, Biomembr. 1858*, 824−835.
(18) Nissen-Meyer, J., Oppegård, C., Rogne, P., Haugen, H. S., and Kristiansen, P. E. (2010) Structure and mode-of-action of the two-peptide (class-IIb) bacteriocins. *Probiotics Antimicrob. Proteins 2*, 52−60.
(19) Oppegård, C., Schmidt, J., Kristiansen, P. E., and Nissen-Meyer, J. (2008) Mutational analysis of putative helix-helix interacting GxxxG-motifs and tryptophan residues in the two-peptide bacteriocin lactococcin G. *Biochemistry 47*, 5242−5249.
(20) Senes, A., Engel, D. E., and DeGrado, W. F. (2004) Folding of helical membrane proteins: the role of polar, GxxxG-like and proline motifs. *Curr. Opin. Struct. Biol. 14*, 465−479.
(21) Schneider, D., and Engelman, D. M. (2004) Motifs of two small residues can assist but are not sufficient to mediate transmembrane helix interactions. *J. Mol. Biol. 343*, 799−804.
(22) Kleiger, G., Grothe, R., Mallick, P., and Eisenberg, D. (2002) GXXXG and AXXXA: common alpha-helical interaction motifs in proteins, particularly in extremophiles. *Biochemistry 41*, 5990−5997.
(23) Teese, M. G., and Langosch, D. (2015) Role of GxxxG motifs in transmembrane domain interactions. *Biochemistry 54*, 5125−5135.
(24) Soliman, W., Wang, L., Bhattacharjee, S., and Kaur, K. (2011) Structure-activity relationships of an antimicrobial peptide plantaricin S from two-peptide class IIb bacteriocins. *J. Med. Chem. 54*, 2399−2408.
(25) Zendo, T., Koga, S., Shigeri, Y., Nakayama, J., and Sonomoto, K. (2006) Lactococcin Q, a novel two-peptide bacteriocin produced by *Lactococcus lactis* QU 4. *Appl. Environ. Microbiol. 72*, 3383−3389.
(26) Oppegård, C., Fimland, G., Thorbæk, L., and Nissen-Meyer, J. (2007) Analysis of the two-peptide bacteriocins lactococcin G and enterocin 1071 by site-directed mutagenesis. *Appl. Environ. Microbiol. 73*, 2931−2938.
(27) Axelsson, L., and Holck, A. (1995) The genes involved in production of and immunity to sakacin A, a bacteriocin from *Lactobacillus sake* Lb706. *J. Bacteriol. 177*, 2125−2137.
(28) Axelsson, L., Katla, T., Bjørnslett, M., Eijsink, V. G. H., and Holck, A. (1998) A system for heterologous expression of bacteriocins in *Lactobacillus sake*. *FEMS Microbiol. Lett. 168*, 137−143.
(29) Ho, S. N., Hunt, H. D., Horton, R. M., Pullen, J. K., and Pease, L. R. (1989) Site-directed mutagenesis by overlap extension using the polymerase chain reaction. *Gene 77*, 51−59.
(30) Sambrook, J., Fritsch, E. F., and Maniatis, T. (1989) In *Molecular Cloning: A Laboratory Manual*, 2nd ed., pp 1.82−81.84, Cold Spring Harbor Laboratory Press, Cold Spring Harbor, NY.
(31) © Agilent Technologies, I. (2009) QuikChange Site-Directed Mutagenesis Kit. Instruction manual.
(32) Aukrust, T. W., Brurberg, M. B., and Nes, I. F. (1995) Transformation of *Lactobacillus* by electroporation, in *Methods in Molecular Biology; Electroporation Protocols for Microorganisms* (Nickoloff, J. A., Ed.), pp 201−208, Humana Press Inc, New York.
(33) Uteng, M., Hauge, H. H., Brondz, I., Nissen-Meyer, J., and Fimland, G. (2002) Rapid two-step procedure for large-scale purification of pediocin-like bacteriocins and other cationic antimicrobial peptides from complex culture medium. *Appl. Environ. Microbiol. 68*, 952−956.
(34) Edebo, L. (1960) A new press for the disruption of microorganisms and other cells. *J. Biochem. Microbiol. Technol. Eng. 2*, 453−479.
(35) Nissen-Meyer, J., Holo, H., Håvarstein, L. S., Sletten, K., and Nes, I. F. (1992) A novel lactococcal bacteriocin whose activity depends on the complementary action of two peptides. *J. Bacteriol. 174*, 5686−5692.
(36) Güntert, P., Mumenthaler, C., and Wuthrich, K. (1997) Torsion angle dynamics for NMR structure calculation with the new program DYANA. *J. Mol. Biol. 273*, 283−298.
(37) Senes, A., Ubarretxena-Belandia, I., and Engelman, D. M. (2001) The Cα—H···O hydrogen bond: a determinant of stability and specificity in transmembrane helix interactions. *Proc. Natl. Acad. Sci. U. S. A. 98*, 9056−9061.
(38) Cheng, X., Jo, S., Lee, H. S., Klauda, J. B., and Im, W. (2013) CHARMM-GUI micelle builder for pure/mixed micelle and protein/micelle complex systems. *J. Chem. Inf. Model. 53*, 2171−2180.
(39) Humphrey, W., Dalke, A., and Schulten, K. (1996) VMD: visual molecular dynamics. *J. Mol. Graphics 14*, 33−38.
(40) Phillips, J. C., Braun, R., Wang, W., Gumbart, J., Tajkhorshid, E., Villa, E., Chipot, C., Skeel, R. D., Kale, L., and Schulten, K. (2005) Scalable molecular dynamics with NAMD. *J. Comput. Chem. 26*, 1781−1802.
(41) Klauda, J. B., Venable, R. M., Freites, J. A., O'Connor, J. W., Tobias, D. J., Mondragon-Ramirez, C., Vorobyov, I., MacKerell, A. D., Jr., and Pastor, R. W. (2010) Update of the CHARMM all-atom additive force field for lipids: validation on six lipid types. *J. Phys. Chem. B 114*, 7830−7843.
(42) Fimland, G., Eijsink, V. G., and Nissen-Meyer, J. (2002) Mutational analysis of the role of tryptophan residues in an antimicrobial peptide. *Biochemistry 41*, 9508−9515.
(43) Fimland, G., Johnsen, L., Axelsson, L., Brurberg, M. B., Nes, I. F., Eijsink, V. G., and Nissen-Meyer, J. (2000) A C-terminal disulfide bridge in pediocin-like bacteriocins renders bacteriocin activity less temperature dependent and is a major determinant of the antimicrobial spectrum. *J. Bacteriol. 182*, 2643−2648.
(44) Kazazic, M., Nissen-Meyer, J., and Fimland, G. (2002) Mutational analysis of the role of charged residues in target-cell binding, potency and specificity of the pediocin-like bacteriocin sakacin P. *Microbiology 148*, 2019−2027.
(45) Miller, K. W., Schamber, R., Chen, Y., and Ray, B. (1998) Production of active chimeric pediocin AcH in *Escherichia coli* in the absence of processing and secretion genes from the *Pediococcus pap* operon. *Appl. Environ. Microbiol. 64*, 14−20.
(46) Yau, W.-M., Wimley, W. C., Gawrisch, K., and White, S. H. (1998) The preference of tryptophan for membrane interfaces. *Biochemistry 37*, 14713−14718.
(47) Killian, J. A., and von Heijne, G. (2000) How proteins adapt to a membrane-water interface. *Trends Biochem. Sci. 25*, 429−434.
(48) de Planque, M. R., Kruijtzer, J. A., Liskamp, R. M., Marsh, D., Greathouse, D. V., Koeppe, R. E., de Kruijff, B., and Killian, J. A. (1999) Different membrane anchoring positions of tryptophan and lysine in synthetic transmembrane alpha-helical peptides. *J. Biol. Chem. 274*, 20839−20846.
(49) Sanchez, K. M., Kang, G., Wu, B., and Kim, J. E. (2011) Tryptophan-lipid interactions in membrane protein folding probed by ultraviolet resonance Raman and fluorescence spectroscopy. *Biophys. J. 100*, 2121−2130.
(50) Adamian, L., and Liang, J. (2002) Interhelical hydrogen bonds and spatial motifs in membrane proteins: polar clamps and serine zippers. *Proteins: Struct., Funct., Genet. 47*, 209−218.
(51) Peter, B., Polyansky, A. A., Fanucchi, S., and Dirr, H. W. (2014) A Lys-Trp cation-pi interaction mediates the dimerization and function of the chloride intracellular channel protein 1 transmembrane domain. *Biochemistry 53*, 57−67.

DOI: 10.1021/acs.biochem.6b00588
Biochemistry 2016, 55, 5106−5116